Physics of the Earth and Planetary Interiors 214 (2013) 35–52

Contents lists available at SciVerse ScienceDirect

Physics of the Earth and Planetary Interiors

journal homepage: www.elsevier.com/locate/pepi

Three-dimensional thermomechanical modeling of oceanic spreading initiation and evolution

Taras V. Gerya

Institute of Geophysics, ETH Zürich, Sonneggstrasse 5, 8092 Zürich, Switzerland

A R T I C L E   I N F O

Article history:
Received 8 May 2012
Received in revised form 2 October 2012
Accepted 18 October 2012
Available online 29 October 2012
Edited by Mark Jellinek

Keywords:
Mid-ocean ridge
Transform fault
Rifting
Oceanic crust growth

A B S T R A C T

This work employs high-resolution 3D thermomechanical numerical models of the incipient oceanic spreading to investigate nucleation and long-term evolution of ridge-transform spreading patterns. The Eulerian–Lagrangian visco-plastic model allows for large strains and accounts for plate cooling by both heat conduction and hydrothermal circulation as well as for partial melting of the asthenosphere and oceanic crust growth by magmatic accretion. According to the numerical experiments, the oceanic spreading pattern depends strongly on the initial offset of spreading centers and the magnitude of fracture healing rate. Three different characteristic long-term spreading modes are obtained: (1) ridge-transform patterns, (2) single ridges and (3) spreading centers with an intermediate plate. Ridge-transform oceanic spreading patterns form gradually from moderate initial offsets of 40–60 km and become fully established several million years after the plate breakup. Moreover, it is demonstrated on the basis of simple analyses that the ridge-transform system is a long-term plate growth pattern that is generally different from an initial plate rifting pattern. Geometry of the ridge-transform system is governed by geometrical requirements (180° rotational symmetry for open space occupation) for simultaneous accretion and displacement of new plate material within two offset spreading centers connected by a sustaining rheologically weak transform fault. According to these requirements, the characteristic spreading-parallel orientation of oceanic transform faults is the only thermomechanically consistent steady state orientation. Results of numerical experiments compare well with both incipient and mature ridge-transform systems observed in nature.

1. Introduction

The characteristic pattern of mid-ocean ridges, sectioned by transform faults stands as an inherent feature of terrestrial plate tectonics. A fundamental unresolved problem is how this pattern formed and why it is maintained. One common view is that oceanic transform faults are typically inherited from the continental plate breakup (e.g., Wilson, 1965; Lister et al., 1986; Cochran and Martinez, 1988; McClay and Khalil, 1998). This view is, in particular, based on a geometric correspondence between passive margins and mid-ocean ridges, which is especially prominent for the South Atlantic Ridge and the West African coast. Several lines of evidence support this view by showing that stepping half-grabens (Cochran and Martinez, 1988; McClay and Khalil, 1998), segmented gravity and magnetic anomalies (Behn and Lin, 2000), or segmented weak regions (Watts and Stewart, 1998) along passive margins lead to the formation of transform faults. Indeed, Lister et al. (1986) proposed that passive margins are characterized by an orthogonal set of normal and transfer faults; the latter potentially developing into transform faults. In contrast, a number of other observations suggest that the characteristic orthogonal ridge – transform fault pattern is not directly inherited from the earlier rift geometry and a one-to-one correspondence between the transfer faults in the continental rift stage and transform faults in the oceanic spreading stage does not exist (Bosworth, 1986; Taylor et al., 1995, 2009). Bosworth (1986) and Rosendahl (1987), amongst others, proposed that half grabens, delimited along strike by accommodation zones, are the fundamental units of rift architecture. Accommodation zones are generally oblique features (Bosworth, 1986; Jarrige et al., 1990), making them unlikely precursors of transform faults (Bosworth, 1986). In addition, high-resolution bathymetry data from the incipient oceanic spreading regions, such as Woodlark Basin, Gulf of Aden and NW Australia, show that spreading segments nucleate en echelon in overlapping rift basins and that initial spreading offsets, where present, are often non-transform (Taylor et al., 1995, 2009). Thus, an ambiguity remains on how the transform faults originated and when, how and why did the orthogonal ridge-transform fault pattern form.

Due to the limited availability of data, detailed interpretations of nucleation and evolution of ridge-transform oceanic spreading patterns are difficult and controversial (Lister et al., 1986; Bosworth, 1986; Dauteuil and Brun, 1996; Taylor et al., 1995, 2009),

E-mail address: taras.gerya@erdw.ethz.ch

0031-9201/$ - see front matter © 2012 Elsevier B.V. All rights reserved.
http://dx.doi.org/10.1016/j.pepi.2012.10.007

thus analogue and numerical models have been employed (see recent review by Gerya, 2012 and references therein). Two main styles of analogue models have been examined: (i) themomechanical freezing wax models with accreting and cooling plates (Oldenburg and Brune, 1972; O'Bryan et al., 1975; Ragnarsson et al., 1996; Katz et al., 2005) and (ii) mechanical models with viscous mantle and brittle lithosphere (Dauteuil and Brun, 1993; Dauteuil et al., 2002; Marques et al., 2007; Tentler and Acocella, 2010). The freezing wax models reproduced characteristic orthogonal ridge – transform fault patterns but often produced open spreading centers with exposed liquid wax, which is dissimilar to nature. On the other hand, in the mechanical models, new lithosphere is not accreted in spreading centers, which is incompatible with oceanic spreading. Also, the rheological properties of the materials used in thermomechanical and mechanical analogue models are highly simplified compared to the temperature-, pressure- and stress-dependent visco-elasto-plastic rheology of multi-phase oceanic lithosphere (e.g., Ranalli, 1995; Buck et al., 2005) subjected to spontaneous weakening and shear-localization in a wide range of P-T conditions (e.g., Bercovici and Ricard, 2012).

Numerical models of transform fault nucleation (Hieronymus, 2004; Choi et al., 2008) and continental rifting (Allken et al., 2011, 2012) mostly focused on spontaneous plate fragmentation (rifting) processes and demonstrated that orthogonal and oblique ridge-transform linkage patterns can spontaneously arise from small, initially offset perturbations (weak seeds) in the plate structure. It was shown numerically with 2D mechanical models (Hieronymus, 2004) that in this case only five fundamental spreading modes can form: orthogonal transform faults, microplates, overlapping spreading centers, zigzag ridges and oblique connecting spreading centers. It was also demonstrated using 3D visco-elasto-plastic thermomechanical models (Choi et al., 2008) that under condition of variable ratio of thermal stress to spreading-induced stress, the orthogonal pattern marks transition from the overlapping to the connecting mode. Based on 3D visco-plastic mechanical models employing a plastic rheology with strain softening, Allken et al. (2011, 2012) indicated that rift offset and viscosity of the lower crust are the main controls on the efficiency of rift propagation and the style of rift segment interaction during continental rifting. Indeed, strain reached in previous numerical experiments was too small to test the evolution of ridge-transform patterns during long-term spreading associated with significant plate accretion. Recent large-strain numerical experiments (Gerya, 2010a) focused on spontaneous nucleation of transform faults at a single straight ridge but the initiation and long-term evolution of ridge-transform oceanic spreading patterns after plate breakup remained unaddressed.

In the present paper we build on the results of previous numerical experiments to develop 3D thermomechanical numerical model of long-term oceanic spreading starting from the culminating stages of continental rifting. The principal goal of this study is to model the dynamics of an incipient spreading process and understand when, how and why typical ridge-transform spreading patterns can be established during the history of oceanic spreading.

2. Numerical model

This work employs high-resolution 3D thermomechanical numerical models of the incipient oceanic spreading to investigate nucleation and evolution of ridge-transform oceanic spreading patterns. The Eulerian–Lagrangian visco-plastic model with an internal free surface (Fig. 1) allows for large strains and spontaneous oceanic crust growth by magmatic accretion. The employed numerical technique (Gerya, 2010a,b) is based on a combination of a finite difference method applied on a uniformly spaced staggered finite difference grid, with the marker-in-cell technique.

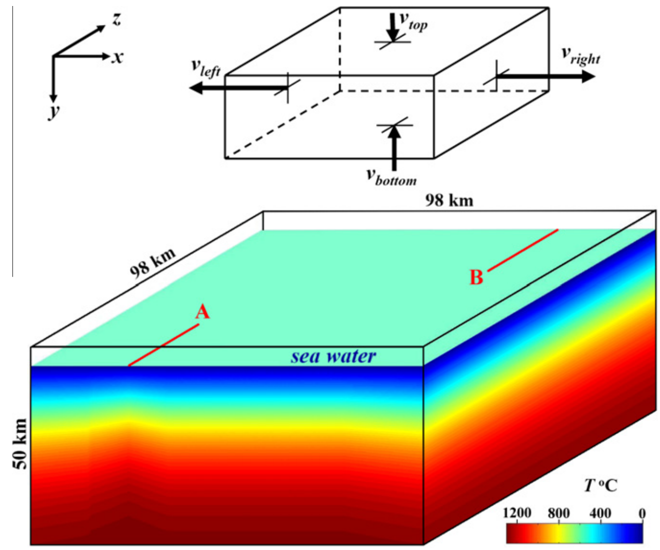

Fig. 1. Initial model setup and boundary conditions for 3D thermomechanical numerical experiments. Boundary conditions are constant spreading rate in x-direction ($v_{spreading} = v_{left} + v_{right}$, where $v_{left} = v_{right}$) and compensating vertical influx velocities through the upper and lower boundaries (v_{top} and v_{bottom}) are chosen to ensure conservation of volume of the model domain and constant average 5 km thickness of the sea water layer [$(v_{top} + v_{bottom})/50 = (v_{left} + v_{right})/98$), where $v_{top}/5 = v_{bottom}/45$]; front and back boundaries in the x-y plane are free slip. A water-loaded free surface condition for the upper plate boundary is implemented by using a weak layer approach (e.g., Schmeling et al., 2008; Gerya, 2010b; Crameri et al., 2012): the weak 5 km thick sea water layer has a characteristic density of 1000 kg/m^3 and a viscosity of 10^{18} Pa s to ensure small stresses (<10^5 Pa) along the upper plate interface. The symmetric initial thermal structure is perturbed in two places where offset linear thermal anomalies (weak seeds) A and B are prescribed by gently elevated geotherm. Thermal boundary conditions are insulating (zero heat flux) on all boundaries with except of the upper and lower boundaries, over which a constant temperature of 273 and 1600 K is prescribed, respectively.

2.1. Model setup

The initial model setup corresponds to the onset of oceanic spreading along an already thinned, idealized rifted margin with a 7–20 km thick crust (Table 1). Similarly to previous numerical models of spontaneous plate fragmentation (e.g., Hieronymus, 2004; Choi et al., 2008; Allken et al., 2011, 2012), two linear thermal perturbations (weak seeds) with an offset of 30–60 km are imposed at the bottom of the lithospheric mantle (Fig. 1). Prescribing of offset perturbations (weak seeds) is a standard approach for both analogue and numerical models of rifting and spreading (e.g., Hieronymus, 2004; Choi et al., 2008; Tentler and Acocella, 2010; Allken et al., 2011, 2012). This approach is consistent with observations on incipient oceanic spreading regions where spreading segments nucleate en echelon in overlapping rift basins with non-transform spreading offsets (Taylor et al., 1995, 2009). The magnitude of the offsets varies in nature and is often in the range of several tens of kilometers (e.g., Bosworth, 1986; Taylor et al., 1995, 2009). In our model the initially offset thermal perturbations affect (but not strictly define) positions of the individual spreading centers. It should also be mentioned that both linear and point-like weak seeds trigger nucleation of elongated rift structures which are nearly orthogonal to the extension direction (e.g., Hieronymus, 2004; Choi et al., 2008; Tentler and Acocella, 2010; Allken et al., 2011, 2012).The modeled (full) spreading rates ($v_{spreading}$) range from 3.8 to 5.7 cm/yr, which simulates incipient slow- to intermediate-spreading ridge (Taylor et al., 2009). The Eulerian computational domain is equivalent to 98 × 98 × 50 km (Fig. 1) and is resolved with a regular rectangular grid of 197 × 197 × 101 nodes and contains 34 million randomly distributed Lagrangian markers. Larger 202 × 98 × 50 km models with 405 × 197 × 101 nodes and